Effects of the Composition and Nematic–Isotropic Phase Transition on the Electro-Optical Responses of Unaligned Polymer-Dispersed Liquid Crystals. I. Composites of Poly(methyl methacrylate) and E8

R. R. Deshmukh, M. K. Malik

Department of Physics, Institute of Chemical Technology, University of Mumbai, Matunga, Mumbai 400 019, India

Received 16 October 2007; accepted 26 December 2007
DOI 10.1002/app.27906
Published online 27 February 2008 in Wiley InterScience (www.interscience.wiley.com).

ABSTRACT: Composite films composed of poly(methyl methacrylate) (PMMA) and the nematic-type liquid crystal (LC) E8 were prepared by solution casting in chloroform. The electro-optical performance characteristics were studied for a wide range of PMMA/E8 compositions (10–80 wt % E8). At two specific levels of LC (70 and 80 wt %), the effects of temperature, voltage, and frequency of the applied electric field on the optical transmittance of films were extensively measured with a He–Ne laser (λ = 632.8 nm) as a light source. Scanning electron microscopy observations showed the formation of large E8 droplets in PMMA due to phase separation, and the homogeneous distribution increased with increasing E8 content. The results were interpreted in terms of aggregation structure, interfacial interaction, LC loading, and the solubility of LC in the polymer matrix. The results obtained indicate that under the experimental conditions imposed, the output could be continuously controlled to the desired level by the selection of a suitable loading of LC to prepare polymer-dispersed LC electro-optical active composite films with response times on the order of only a few milliseconds. © 2008 Wiley Periodicals, Inc. J Appl Polym Sci 108: 3063–3072, 2008

Key words: PDLC; composites; phase separation; electro-optical; nematic liquid crystal

INTRODUCTION

Polymer-dispersed liquid crystal (PDLC) films have gained tremendous importance during the last 2 decades for use in electro-optical devices ranging from light shutters and switchable windows to high-resolution large-area displays, projection light valves, and switching gratings.[1–7] PDLCs are usually composed of microsized droplets of liquid crystals (LCs) randomly dispersed in a polymer matrix and are formed by the phase separation of the LC component from a homogeneous solution with a polymer or a prepolymer.[8] The polymer matrix, consisting of LC droplets, is sandwiched between two glass slides with a transparent conductive substrate such as indium tin oxide (ITO). This resulting assembly forms an electrosensitive material that can be switched from a light-scattering state (off state) to a transparent state (on state) by the application of an external electric field (E) or thermal gradient.[9–11] These functional responses are highly dependent on the optical microstructural heterogeneities and/or homogeneities of the composite film. The surface anchoring causes a nonuniform director field within these droplets, which results in the mismatch between the ordinary refractive index of the liquid crystal (n_o) and the refractive index of the polymer matrix (n_p).

Various methods, such as thermally induced phase separation, solvent-induced phase separation (SIPS), polymerization-induced phase separation, and encapsulation, can be used to prepare PDLC films.[12] In this study, we used the SIPS method where the LC and the polymer are dissolved in a common solvent to create a single phase. As the solvent evaporation takes place, the LC phase separates into droplets or domains surrounded by polymer walls. The distortion of the nematic director (n) in the LC droplets, which has a profound effect on the high scattering and switching properties of PDLC films, strongly depends on the aggregation structure, which can be controlled on the basis of the solvent evaporation rate and LC ratio during the film preparation process.[13–15] Drzaic[12] investigated the effect of domain size on the switching field and showed that this field is inversely proportional to the average domain size and to the domain anisotropy.

In this study, we fabricated several PDLC films based on poly(methyl methacrylate) (PMMA)/E8 to study their morphology and electro-optical light

Correspondence to: R. R. Deshmukh (rajedeshmukh@rediffmail.com).

Contract grant sponsor: Board of College and University Development (BCUD), University of Mumbai.

Journal of Applied Polymer Science, Vol. 108, 3063–3072 (2008)

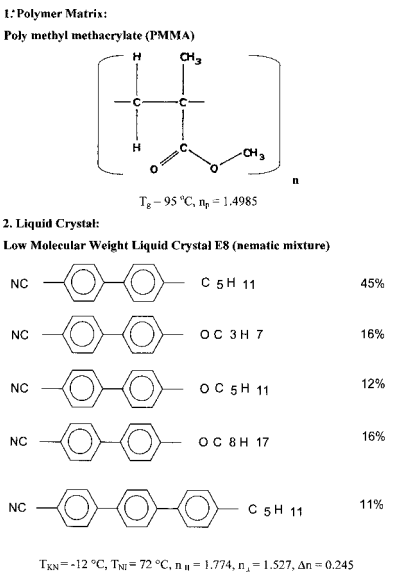

Figure 1 Chemical structures and physical properties of the constituents: (1) PMMA and (2) E8. T_g, glass transition temperature; T_{KN}, solid to nematic phase transition temperature; $n_{\prod}$, extraordinary refractive index; $n_{\perp}$, ordinary refractive index.

scattering behavior on the basis of the aggregation structures and the effect of LC domain size on electro-optical properties such as threshold voltage (V_{th}), driving field, and response time (RT). Furthermore, we studied the optical and electro-optical responses of these films as a function of temperature, and the results show an enhancement in these properties. We also describe the observed hysteresis in transmission at room temperature and the semimemory effect at higher temperatures. The possible mechanisms are discussed in terms of an interfacial interaction between the polymer matrix and the LC molecules.

EXPERIMENTAL

Materials

The nematic LC E8 (kindly provided by E. Merck, Darmstadt, Germany) used in this study was a eutectic mixture of a number of cynophenyl derivatives with positive dielectric anisotropy ($\Delta\varepsilon$). E8 was thermotropic in nature. The polymer was PMMA. The chemical structures and physical properties of these constituents are given in Figure 1.

Preparation of the PDLC composite films

In this study, PDLC films with different compositions (wt/wt %) of polymer and LC were prepared by the SIPS method.[16,17] We prepared a homogeneous solution of an appropriate amount of PMMA and E8 in chloroform (solvent) by spreading it on ITO-coated glass as a substrate at room temperature (25°C). The glass plate was kept floating on mercury to get a uniformly thick film. The solvent evaporation rate during film preparation was controlled by regulation of the pressure in the chamber with a needle valve and a vacuum pump, mainly to get LC-induced aggregation structures in the polymer matrix. Another ITO-coated glass plate was used for sandwiching the PDLC films. Film thickness was controlled with a poly(ethylene terephthalate) film spacer 18 μm thick. There were no alignment layers on the cell substrates.

During preparation, the composite films with E8 content greater than 80 wt % showed poor adhesion to the substrate as the entire amount of E8 could not be held in the micropores of PMMA; hence, these were not studied. Similar observations were reported by Miyamoto et al.[18]

Morphology

The morphology of the PDLC composite films were studied with a scanning electron microscope (Philips XL 30, Eindhoven, The Netherlands). For structural studies, E8 was first extracted from the films with methanol, which is a nonsolvent for PMMA, and then, these films were dried overnight *in vacuo* before they were viewed by scanning electron microscopy (SEM).

Electro-optical measurements

The electro-optical properties of the prepared PDLC films were studied in terms of transmission changes with a driving alternating-current (ac) frequency. The experimental system is shown schematically in Figure 2. A collimated beam of a He–Ne laser (wavelength = 632.8 nm with 10 mW power; Photochemical, Inc., Canada; model 105P) was used as an incident light source. An ac *E* was provided by amplification of the signal (50 Hz to 1 kHz square waves) from a function generator and its application to the conductive electrodes (ITO-coated glass plates). The voltage was increased in steps of 10 V from 0 to 300 V during the scan-up cycle to drive the PDLC films and was decreased (scan-down cycle) in the same way to 0 V. Between all of the subsequent cycles, the PDLC films were kept for 5 min in the off state. The transmitted light intensity without any polarizer was measured in its normal transmission geometry through a photodiode (Jain-Laser Tech, Mumbai, India). The distance between the PDLC film and the photodiode was 300 mm. The response of the photodiode was monitored with a digital storage type oscilloscope (Tektronix TDS 430A, 400 MHz, Beaverton, OR). We introduced an oven system in the same setup to measure the temperature dependence of transmission for these PDLC films. A temperature

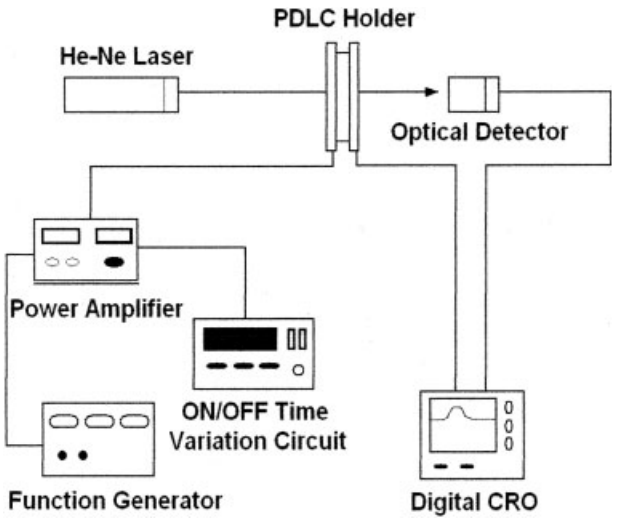

Figure 2 Experimental setup for electro-optical measurements. CRO, cathode ray oscilloscope.

controller with an accuracy of ±0.5°C with a heating rate as low as 0.5°C/min was used. Because of the thermal properties of the materials used, a heating rate of 2°C/min was used throughout.

RESULTS AND DISCUSSION

Effect of the LC content

Figure 3 shows off- and on-state (50 Hz, 200 Vp-p) transmissions of the PMMA films with various E8 contents at 25°C. Vp-p is defined as peak to peak voltage of the applied signal. The main consideration of this experiment was to obtain optimized composite films in terms of maximum optical contrast. The strong light intensity contrast (difference in the transmittance of the cell with and without applied *E*) appeared in the range 70–80 wt % E8. If we considered the composites for optical applications, these films were the most valuable, and hence, the electro-optical responses with ac electric voltages were studied for these two compositions.

Morphology

The degree of light scattering in the PDLC composite films greatly depended on the LC aggregation states. It was important to have LC domains of a size comparable to the wavelength of visible light for strong light scattering. Another factor that greatly affected the opacity of these devices was the distribution of these phase-separated LC droplets. A high LC content left a small volume of the polymer unoccupied, which hence increased light scattering. The most stable structure in the nematic phase was known by a uniform distribution of bipolar shaped droplets, but certain variations could rise due to a restriction of these droplets to spherical voids. This aggregation structure of LC droplets depends on a number of factors, such as the types of polymer and LC used, their anchoring at interface, composition and elastic properties, and in particular, the details of the film-forming procedure.[4] In SIPS, solvent evaporation plays a major role in the determination of the final aggregation structure of the composite films. In this technique, small LC domains are formed upon solvent evaporation, followed by the coalescence of these small domains to form larger ones. The process eventually leads to the formation of interconnected LC channels when the LC loading is high enough. A fast evaporation rate of solvent will result in the quick solidification of polymer, which will lead to a considerable amount of LC residing in it as an unseparated phase and will result in the formation of small-size LC domains. A slow evaporation rate will significantly increase immiscibility between polymer and LC and thus allow the LC phase to separate efficiently and form a large number of LC domains.

Figure 4 shows the SEM micrographs obtained from the PMMA/E8 composite films (30/70 and 20/80 wt %) after the removal of E8. The weight loss upon extraction could be used to decide the continuity of the LC domains in the polymer matrix. As the weight change of the composite films after the extraction of E8 almost corresponded to the loaded E8 weight fraction, this clearly indicated that almost all of the LC fraction was able to be extracted. Here, the droplet size ranged from submicrometers to several micrometers. With a LC content of 70 wt %, the micrograph showed large elongated LC cavities embedded in the three dimensions as a continuous phase and separated by the PMMA matrix polymer walls, which formed a three-dimensional spongy network. It was apparent that a few droplets interconnected to form larger ones, which gave rise to variation in the droplet size. As the LC content increased to 80 wt %, a better coalescing morphology

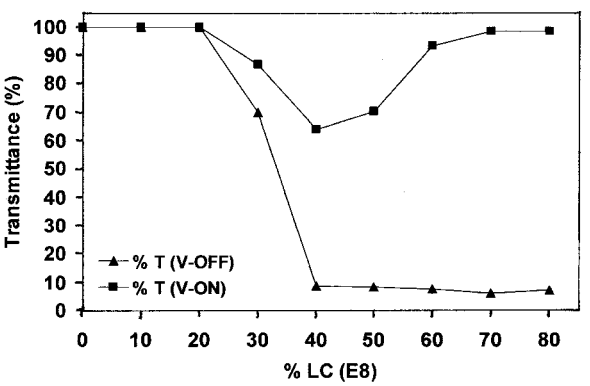

Figure 3 Optical contrast of the PMMA/E8 composite films versus the LC content (V-ON corresponds to 50 Hz, 200 Vp-p and V-OFF corresponds to no applied field).

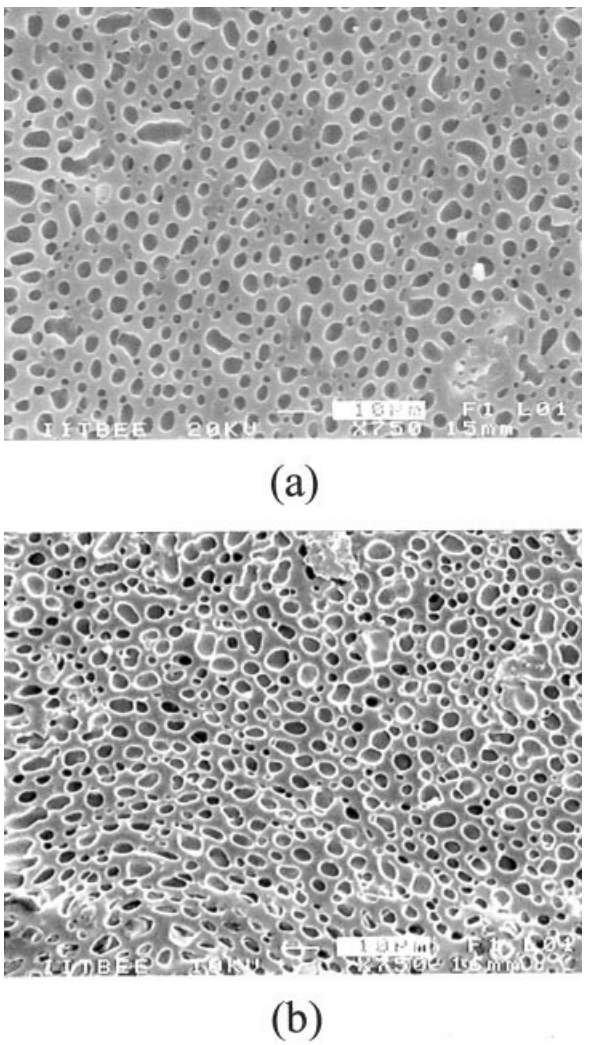

Figure 4 SEM micrographs of the PMMA/E8 films: (a) 30/70 and (b) 20/80 wt %.

with relatively large voids in the structure of polymer network was observed, where droplets became large and more elongated and occupied a large volume of PMMA. These droplet cavities, in general, were very large and spheroid in shape with the major axis lying parallel to the film base. With such morphologies, it seems reasonable to consider that these composite films of 30/70 and 20/80 wt % compositions formed a suitable microstructure for electro-optical effects and could be treated as binary dielectrics with the polymer matrix and LC as two components.

Electro-optical responses

On the basis of Wu's model,[19] the application of E reoriented the elongated droplet n to its equilibrium orientation (N; Fig. 5). If θ_1 is the angle between the direction of N and E, Wu's model describes θ_1 as

$$\theta_1 = \frac{1}{2}\tan^{-1}\left(\frac{\sin 2\theta_2}{A + \cos 2\theta_2}\right) \quad (1)$$

where θ_1 and θ_2 are defined in Figure 5 and $A = \Delta\varepsilon a^2\varepsilon^2/K(l^2 - 1)$, where ε is the permittivity, a is the major axis of the LC droplet with an assumption that it is an ellipsoid, K is the elastic constant, and $l = (a/b)$, where b is the minor axis of the LC droplet. The equation indicates that the orientation order parameter (N) gradually approaches the direction of E, with increasing field strength in an elongated LC droplet, provided $\Delta\varepsilon$ is positive. In such a situation, the LC molecules in the PDLC film will align with their long molecular axis parallel to the applied field with minimum energy level. According to the model, V_{th}, defined as the voltage required to raise transmission by 10% of the original transmission, for the director reorientation in droplets with a bipolar configuration, which results in a variation of optical transmission of the PDLC system, is determined by the balance between the elastic force, surface interaction, and applied electric force and is given by

$$V_{th} = \frac{d}{3a}\left(\frac{\rho_P}{\rho_{LC}} + 2\right)\left(\frac{k(\ell^2 - 1)}{\Delta\varepsilon}\right)^{1/2} \quad (2)$$

where d is the cell thickness; ρ_P and ρ_{LC} are the resistivities of the polymer and liquid crystal, respectively; ℓ is the aspect ratio (major dimension/minor dimension) of the LC droplet with an assumption that it is an ellipsoid; and $\Delta\varepsilon$ is the dielectric anisotropy of the LC. From eq. (2), it is clear that V_{th} can be reduced by the control of various factors, such as film thickness and resistivity ratio, and by an increase in the size of the droplets. However, dielec-

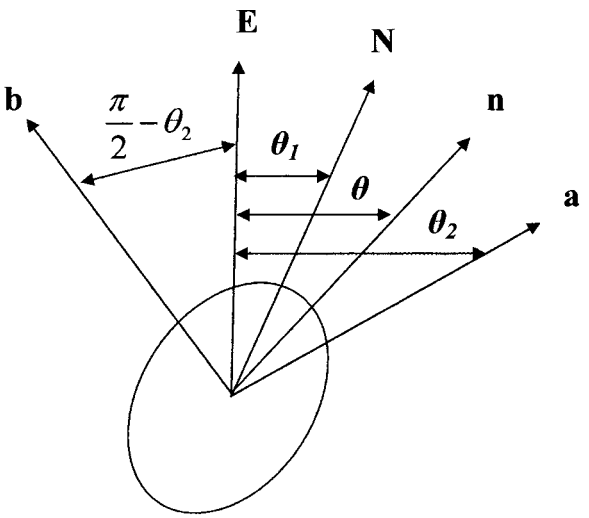

Figure 5 Illustration of the droplet n orientation in an elongated cavity.

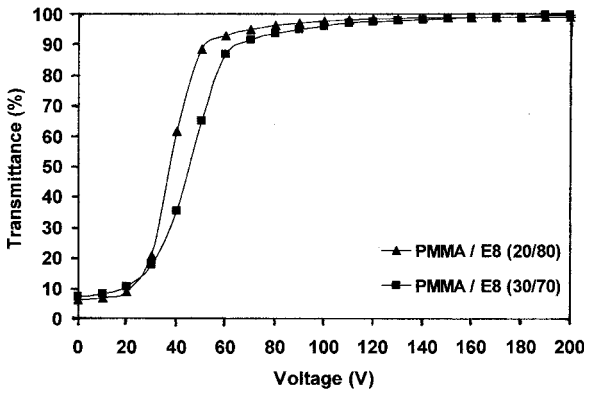

Figure 6 Transmittance versus V for the PMMA/E8 composite films at 200 Hz.

tric studies of various PDLC composite materials have clearly indicated that increasing $\Delta\varepsilon$ by varying the frequency of applied signal plays a major role in lowering the operating V_{th}.[18,20–23]

To analyze the electro-optical behavior of our samples, we measured the transmission variation by changing the amplitude and frequency of the applied E. The applied field was driven by a square-wave voltage with the frequency varied from 50 Hz to 1 kHz, and we found that 200 Hz was the optimum frequency for our samples. The transmittance response with voltage corresponded to high-frequency characteristics. In a low-frequency range (<50 Hz), a periodic flicker of light with twice the imposed frequency overlapping the asymptote was observed.[18] However, in a high-frequency range, the fluctuation of transmitted light was too small to be observed, and the magnitude of transmittance was observed as a monotonous increasing curve. In this case, the time period of the applied field to change its polarity was shorter than that of the LC molecules to change from the homeotropic alignment to spontaneously random orientation.

Figure 6 shows the response curves of transmittance for the PMMA/E8 (20/80 and 30/70 wt %) composite films as a function of applied voltage (V) at 200 Hz. The composite with a higher concentration of polymer required a higher V_{th}. The reason is easily understood because the polymer, as a typical dielectric material, consumed a great part of the V, which led to a reduced effective voltage for the LC. Initially, in both the composite films, transmittance increased slowly with applied field up to 20 V and then increased rapidly up to 80 V, after which it reached a maximum. The observed V_{th} decreased from 28.9 V for the 30/70 wt % composite to 27.3 V for the 20/80 wt % composite at 200 Hz. Figure 4(a,b) clearly demonstrates that the droplet size increased with increasing LC content. This observation also indicated that eq. (2) qualitatively accounted for the composition dependence of V_{th}. When the voltage applied was lower than V_{th}, very little alteration was induced on the LC molecular director. As the amplitude of the applied signal increased, the LC molecules started aligning themselves parallel to the E direction, which thus reduced the mismatch between the refractive indices of the polymer matrix and the LC domains. A complete or maximum matching of refractive indices took place at higher voltage, where light transmission achieved maximum value. This voltage, known as the driving voltage, drove the PDLC films from minimum transmission to maximum transmission and was different for different compositions. We also recorded the switching voltage as the voltage for which transmittance was 90% of the total transmittance change, which was again lowered from 65.35 V for 30/70 wt % to 51.25 V for 20/80 wt %, which indicated that the formation of continuous and elongated three-dimensional LC channels was important for good electro-optical response.

During the study, a well-known hysteresis phenomenon[2] was observed in all our PDLC samples. Hysteresis is often measured by the changing of the applied field across a PDLC film during scan-up and scan-down cycles and comparison of the optical response at each voltage level. A measure of hysteresis is given by the voltage width at half maximum. Figure 7 shows the experimental results measured in this manner. Various sources are known to cause hysteresis effects in PDLCs.[2,24] It was suggested that hysteresis may be related to the mechanism of orientation of the LC droplet director,[25] which ultimately depends on the polymer/LC compatibility induced interfacial polymerization influencing the distribution of relaxation time.[12] Because in this study, the PDLC films were prepared from the SIPS technique, the droplet size was highly influenced by the polymer/LC interaction, and its viscosity and, hence, the droplet-size distribution were broad, as justified by the SEM micrographs shown in Figure 4. Equation (2) clearly shows that the orienting field is inversely proportional the droplet radius. At small voltages, droplets of higher sizes align first, and therefore, the applied field necessary to align a maximum number of LC droplets spans wider intervals during both scan cycles, which gives rise to hysteresis.

Another decisive factor for the evaluation of film performance is its dynamic response to an applied field. It generally depends on the relative strength of the applied field and the elastic reorientation forces. For an elongated droplet, rise time (T_R) is defined as the time required for the transmittance of a PDLC film to change from 10 to 90% when a given voltage is applied, and decay time (T_D) is defined as the time required for transmittance to

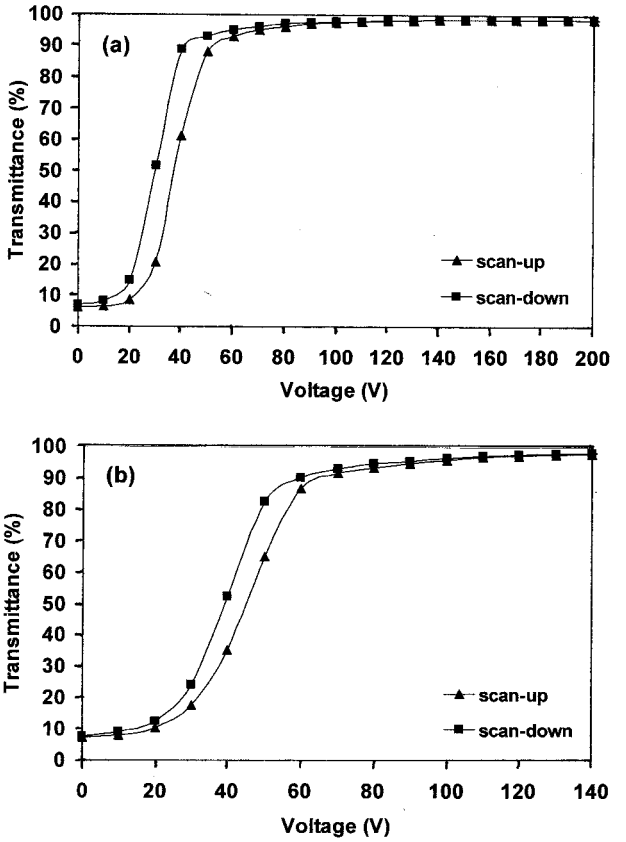

Figure 7 Hysteresis curves for the PMMA/E8 films: (a) 20/80 and (b) 30/70 wt %.

reach 10% when V is removed. These times are given by:[19]

$$\frac{1}{T_R} = \frac{1}{\gamma_1}\left[\Delta\varepsilon \times V^2 - \frac{K(l^2-1)}{a^2}\right] \quad (3)$$

$$T_D = \frac{\gamma_1 \times a^2}{K(l^2-1)} \quad (4)$$

where γ_1 is the rotational viscosity of liquid crystal. RT is defined as the summation of T_R and T_D. An analysis of eqs. (3) and (4) indicates that T_R can be continuously controlled with voltage, whereas T_D does not depend on V but on the LC domain shape, size, and interfacial interaction between the polymer wall and the LC molecules. The latter process is generally slower than the former, and hence, T_R is shorter than T_D. The experimental results for T_R and T_D are displayed in Figures 8 and 9, respectively. The measurements show that the responses are very good when V is higher than 50 V. This result was in good agreement with the transmittance–voltage curves, as shown in Figure 6. A decrease in T_R with increasing voltage was observed for both of the composite films. Moreover, T_R was enhanced as the content of E8 increased, which was mainly due to the increment of LC domains and droplet size, as shown earlier in Figure 4. On the other hand, T_D of these films showed the opposite tendency and was apparently independent of the applied field. As expected, from the figure, it follows that films with a smaller percentage of E8 took less time to decay. This may have been primarily due to the smaller E8 domain morphology. Such a response strongly supported the LC domain size dependence of T_D in eq. (4). However, in both of the composite systems, T_D increased with increasing V, which suggested that the rotation and higher order alignment of LC molecules along the applied E direction occurred at a higher driving voltage. This required a much greater distortion of the LC droplet director upon field removal and, in turn, a greater restoration energy.

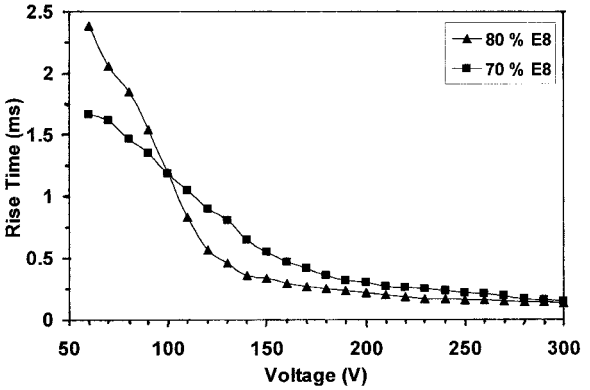

Figure 8 T_R versus V for the PMMA/E8 films with various E8 contents.

Temperature dependence of the transmittance and RT

In practical applications, PDLC-film-based devices are often subjected to a wide range of operating temperatures. It was, therefore, important to study

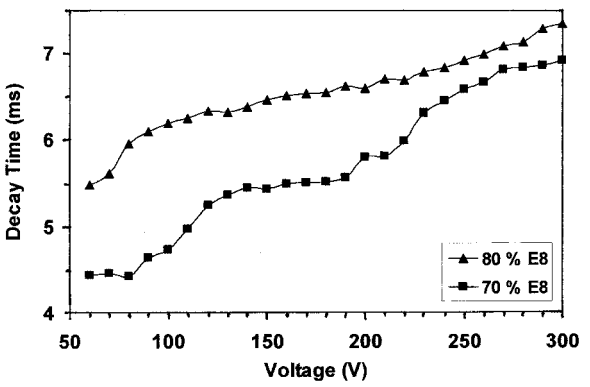

Figure 9 T_D versus V for the PMMA/E8 films with various E8 contents.

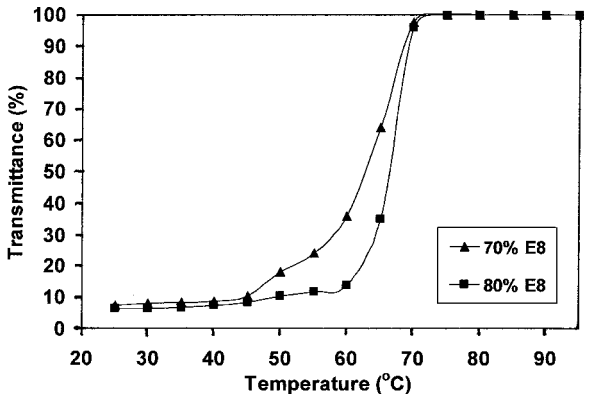

Figure 10 Transmittance as a function of temperature for the PMMA/E8 films with various E8 contents.

the temperature dependence of these transmission characteristics. To observe the thermo-optical behavior of the composites, the temperature was increased without the application of an external E, and the results of this are shown in Figure 10. The transmittance for both of the composites increased with increasing temperature. This temperature dependence of transmittance was closely related to the decrease in birefringence ($\Delta n = n_e - n_o$, where n_e is the extraordinary refractive index) of LC[4,26] and its increased solubility in the polymer matrix.[18] With increasing temperature, n_e decreased along with an increase in n_o, which resulted in an overall decrease in Δn as[26,27]

$$\Delta n \propto \left(1 - \frac{0.98T}{T_{NI}}\right)^{0.22} \quad (5)$$

As a result, the effective refractive index of LC decreased and came very close to n_p, which increased transmittance. As shown in Figure 10, the transmittance of both PDLC films remained almost constant up to a certain temperature, known as the *critical temperature,* and then increased rapidly. A considerable increase in the critical temperature from 45 to 60°C was seen in addition to a steeper response as the E8 content in PMMA was increased from 70 to 80 wt %. This was related to the scattering event of incident light, which is a function of the refractive index differences (1) between a LC droplet and the polymer, (2) between two adjacent droplets, and (3) within a LC droplet. With increasing LC ratio, the number of phase-separated LC droplets increased (Fig. 4), and hence, a high-order scattering of incident light was retained over a long temperature range. Further, at the nematic–isotropic transition temperature (T_{NI}) of E8, the PDLC films became fully transparent. The high transparent state of the films beyond T_{NI} could not be related to the refractive index matching proposition, as there was a relatively considerable difference between the refractive index of both the polymer and LC. Such a transparent state arose due to the dissolution of the LC mixture (in a clear liquid state) in the polymer matrix, which left no scattering sites for incident light.

The electro-optical transmission properties varied significantly with temperature. If only temperature-dependent terms in eq. (2) are considered, according to mean-field theory, V_{th} is proportional to $(K/\Delta\varepsilon)^{1/2}$ with $K \approx S^2$ and $\Delta\varepsilon \approx S$, where S is an order parameter.[28–30] Here, it is assumed that the ratio of the conductivities of the LC and polymer are independent of temperature. As the temperature increases, S of the LCs, which is approximately proportional to $(T/T_{NI})^{-r}$, decreases strongly.[31] Here, r is the critical exponent associated with S and comes to the order of 0.08, T is the temperature, and T_{NI} is the nematic–isotropic transition temperature. Hence, according to the theory

$$V_{th}T^{0.4} \approx \text{Constant} \quad (6)$$

Figure 11 shows the variation in transmittance as a function of applied field for both of the PDLC films at various temperatures. It is immediately observed that eq. (6) was followed appropriately as the threshold field decreased with increasing temperature.

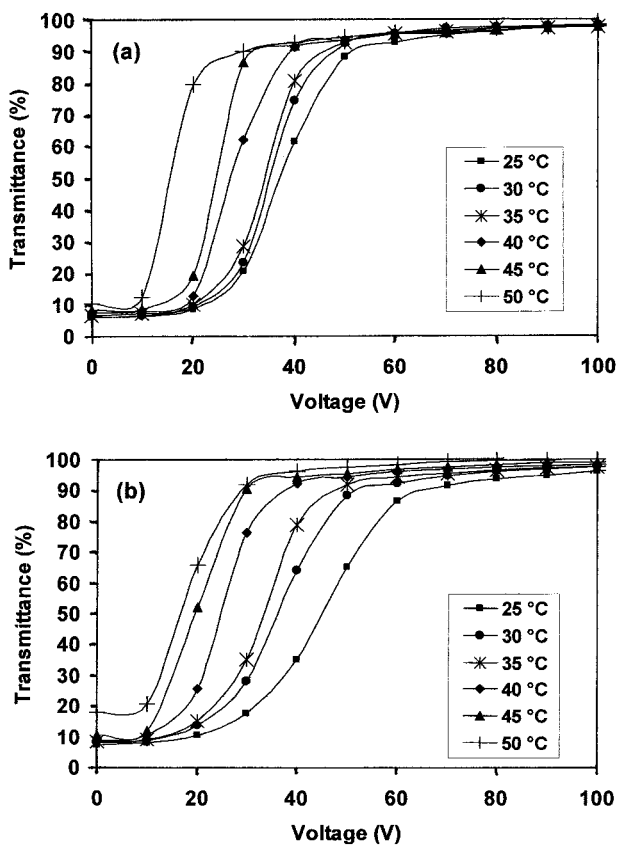

Figure 11 Transmittance versus V at various ambient temperatures for the PMMA/E8 composites: (a) 20/80 and (b) 30/70 wt %.

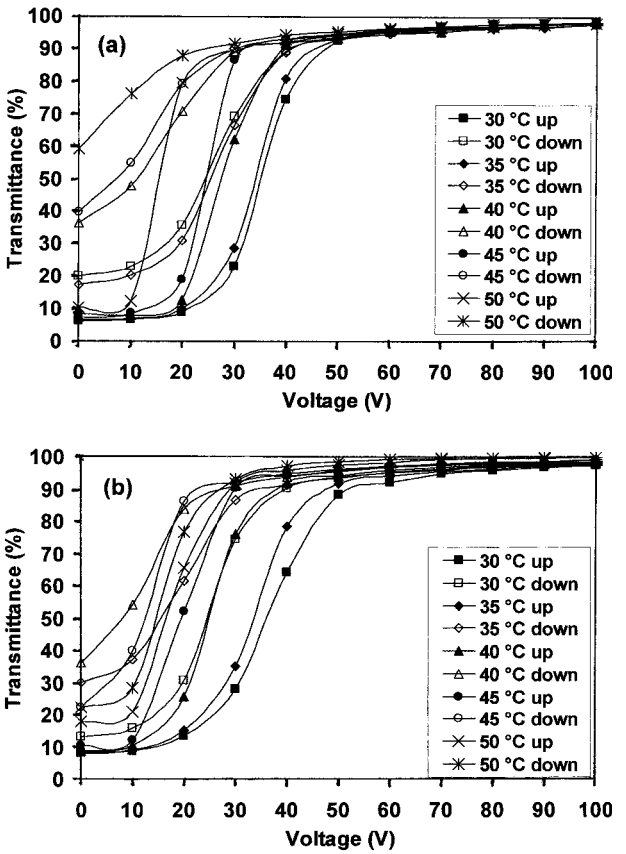

Figure 12 Hysteresis curves at various temperatures for the PMMA/E8 films: (a) 20/80 and (b) 30/70 wt %.

Additionally, the switching and driving fields also decreased as the transmittance curves shifted to lower voltages. According to the mean-field theory proposed by Maier and Saupe,[28] $A = \Delta\varepsilon a^2\varepsilon^2/K(l^2 - 1)$ is approximately proportional to $(T/T_{NI})^{0.7}$, and at higher temperatures, it decreases θ_1 (the angle between direction of N and E) in Wu's model (Fig. 5).[19] Thus, an applied field, even with small amplitude, would reorient the LC droplets sufficiently to satisfy the condition of refractive index matching, and hence, transmittance predominantly becomes a characteristic of low V's with increased temperatures.

Although intensive investigations were made, many areas remain to be more fully studied for the development of reliable and stable PDLC devices. In particular, the effects of temperature on electro-optical hysteresis have rarely been reported. In fact, there is no such evidence for this phenomenon occurring in acrylate systems. Han[32] studied the thermal hysteresis for PDLC film based on NOA61/E7 previously with a low concentration of LC (E7), and the experimental results show that the PDLC films exhibited memory effects that could be erased by the heating of the film above the clearing temperature of LC.[33–36] In this study, we investigated the thermal hysteresis effect, and our results are shown in Figure 12. It is clear that for both of the composite films, the off-state transmittance after the scan-down cycle did not return to its original scattering state, and the films retained some portion of saturating transmission even after the removal of the applied field. However, unlike the memory effect, where a film is in a particular transmission state indefinitely unless heated above the clearing temperature of LC, these composite films took few seconds to return to their original state. Such a phenomenon is known as persistence,[12] where the electro-optical hysteresis extends to zero field.

Figure 13 shows T_R as a function of voltage for both of the composite films at various ambient temperatures. From the figure, it follows that T_R decreased with increasing voltage and temperature. This decrease in T_R was due to the decreased γ_1, which affected its interfacial interaction with the polymer and can be understood in terms of eq. (3). When a saturating E is applied, T_R is expected to scale as γ_1/V^2. Because γ_1 decreased rapidly with increasing temperature, the observed results could be reasonably explained. Furthermore, as shown by the analysis of Wu's model,[19] the dependence of T_R

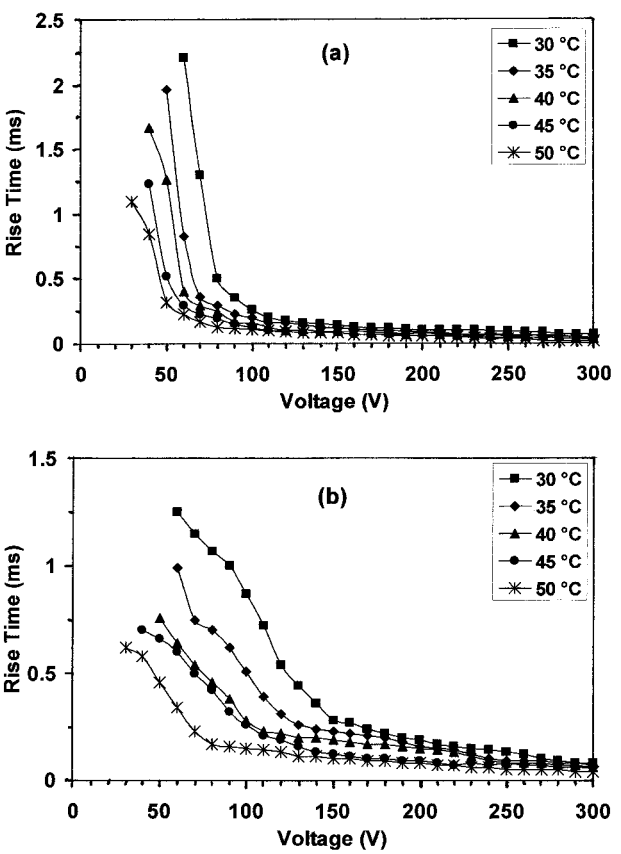

Figure 13 T_R versus V at various temperatures for the PMMA/E8 films: (a) 20/80 and (b) 30/70 wt %.

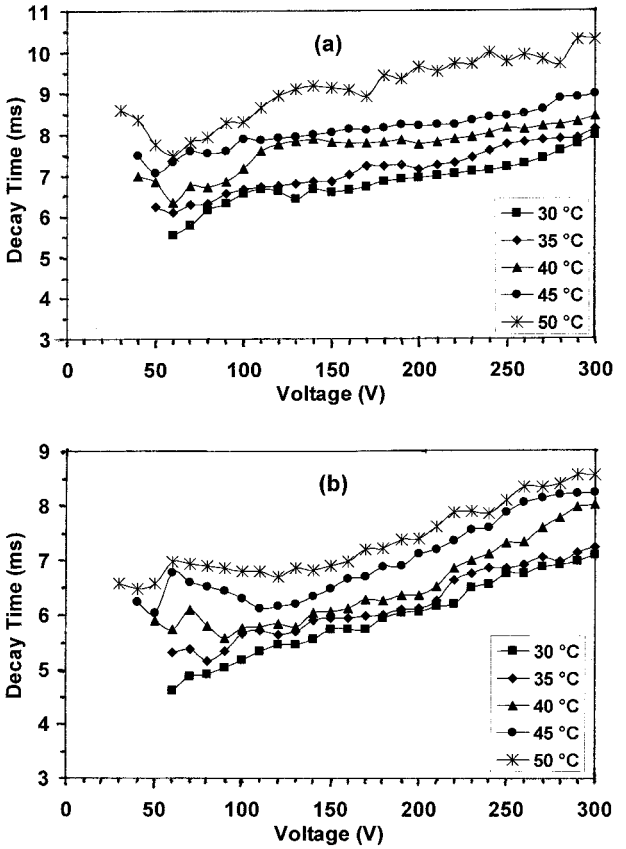

Figure 14 T_D versus V at various temperatures for the PMMA/E8 films: (a) 20/80 and (b) 30/70 wt %.

on V and temperature can be given as $T_R V^2 T^{1.5}$ = Constant. The results given in Figure 13 follow the previous relation approximately.

On the other hand, T_D was approximately proportional to γ_1/K, and according to Wu's model,[19] its dependence on voltage and temperature can be given as $T_D T^{0.8}$ = Constant. Figure 14 shows the T_D measurements as a function of temperature and applied field for both of the composite films. T_D was almost independent of the applied field and strongly depended on the temperature only. In fact, T_D depended on a time constant with $V = 0$. However, the increase in T_D may not be properly explained by the decreased K of LC, as γ_1 also decreased with increasing temperature. The observed increase in T_D with increasing temperature may be understood in terms of the enhanced thermal molecular motion of the polymer chain, which delayed the orientation of LC nematic directions from a homeotropic state to a random orientation state.

CONCLUSIONS

In this study, we examined the temperature dependence of the electro-optical properties of PDLC films composed of a PMMA matrix polymer and the LC E8. It was clear that light transmittance strongly depended on the concentration of LC, where the films with E8 weight fractions of 70 and 80% produced the highest optical contrast. A homogeneous distribution of large phase-separated LC domains occupying a large volume of polymer was seen at these compositions, which caused strong light scattering of the unpowered films. The thermo-optical behavior of these films showed a change in light transmission based on thermal variations. Such a performance could be used to realize temperature sensors. Films containing 80 wt % E8 showed a preferred morphology with better electro-optical responses, such as V_{th}, driving voltage, and T_R, for wide ranges of voltage, frequency, and temperature. These results were closely related to the collective behavior of LC microdroplets, which were larger, elongated, and more uniformly distributed for 80 wt % E8.

The authors thank A. K. Kalkar for helpful discussions and S. A. Bhamre for his technical assistance with the research work.

References

1. Wu, B. G.; West, J. L.; Doane, J. W. J Appl Phys 1987, 62, 3925.
2. Drzaic, P. S. Liq Cryst 1988, 3, 1543.
3. Drzaic, P. S.; Muller, A. Liq Cryst 1989, 5, 1467.
4. Doane, J. W. In Liquid Crystals: Applications and Uses; Bahadur, B., Ed.; World Scientific: Singapore, 1990; Vol. 1.
5. Bowley, C. C.; Crawford, G. P. Appl Phys Lett 2000, 76, 2235.
6. Lee, S. N.; Sprunt, S.; Chien, L. C. Liq Cryst 2001, 28, 637.
7. Senyuk, I.; Smalyukh, I. I.; Lavrentovich, O. D. Opt Lett 2005, 30, 249.
8. Khoo, I. C.; Wu, S. T. Optics and Nonlinear Optics of Liquid Crystals; World Scientific: Singapore, 1993.
9. Ren, Y.; Petti, L.; Mormille, P.; Blau, W. J. J Mod Opt 2001, 48, 1099.
10. Petti, L.; Mormille, P.; Blau, W. J Mol Cryst Liq Cryst 2001, 359, 53.
11. Kayacan, O.; San, S. E.; Okutan, M. Phys A 2007, 377, 523.
12. Drzaic, P. S. Liquid Crystal Dispersions; World Scientific: Singapore, 1995.
13. Kajiyama, T.; Park, K.; Usui, H.; Kikuchi, H.; Takahara, A. Proc SPIE 1993, 122, 1911.
14. Park, K.; Kikuchi, H.; Kajiyama, T. Polym J 1994, 26, 895.
15. Kalkar, A. K.; Kunte, V. V. Mol Cryst Liq Cryst 2002, 383, 1.
16. West, J. L. Mol Cryst Liq Cryst 1988, 157, 427.
17. Kim, B. K.; Ok, Y. S. J Appl Polym Sci 1993, 49, 1769.
18. Miyamoto, A.; Kikuchi, H.; Morimura, Y.; Kajiyama, T. New Polym Mater 1990, 2, 27.
19. Wu, B. G.; Erdmann, J. H.; Doane, J. W. Liq Cryst 1989, 5, 1453.
20. Miyamoto, A.; Kikuchi, H.; Kobayashi, S.; Morimura, Y.; Kajiyama, T. Macromolecules 1991, 24, 3915.
21. Kelly, J.; Seekola, D. Proc SPIE 1990, 7, 1257.
22. Rout, D. K.; Jain, S. C. Mol Cryst Liq Cryst 1992, 210, 75.
23. Kikuchi, H.; Nishiwaki, J.; Kajiyama, T. Polym J 1995, 12, 1246.

24. Reamey, R. H.; Montoya, W.; Wong, A. Proc SPIE 1992, 1665, 2.
25. Kelly, J. R.; Wu, W.; Palffy-Muhoray, P. Mol Cryst Liq Cryst 1994, 243, 11.
26. Vaz, N. A.; Montgomery, G., Jr. J Appl Phys 1987, 62, 3161.
27. Coates, D.; Greenfield, S.; Sage, I. C.; Smith, G. Proc SPIE 1990, 1257, 37.
28. Maier, W.; Saupe, A. Z Naturforsch A 1960, 15, 827.
29. Stephen, M. J.; Straley, J. P. Rev Mod Phys 1974, 46, 617.
30. Gruler, H. Z. Z Naturforsch A 1973, 28, 494.
31. Yakhmi, J. V.; Kelmer, Y. K.; Shukla, R. P.; Manohar, C. Mol Cryst Liq Cryst 1979, 53, 55.
32. Han, J. J Kor Phys Soc 2003, 43, 45.
33. Yamagishi, F. G.; Miller, L. J.; van Ast, C. I. Proc SPIE 1989, 1080, 24.
34. Yamaguchi, R.; Sato, S. Jpn J Appl Phys 1991, 30, 616.
35. Kalkar, A. K.; Kunte, V. V.; Deshpande, A. A. J Appl Polym Sci 1999, 74, 3485.
36. Kato, K.; Tanaka, K.; Tsuru, S.; Sakai, S. Jpn J Appl Phys 1993, 32, 4594.